electrochem

MDPI

Article

Investigation of the Mechanical Properties of Electroless Nickel Coatings Deposited on an ABS Substrate at Different pH Levels

Sabina Cherneva [1,2,*], Dimitar Stoychev [3] and Jennifer Hay [4]

[1] Institute of Mechanics, Bulgarian Academy of Sciences, Acad. G. Bonchev St., B1.4, 1113 Sofia, Bulgaria
[2] National Centre of Excellence Mechatronics and Clean Technologies, Bul. Kliment Ohridski, B1.8, 1756 Sofia, Bulgaria
[3] Institute of Physical Chemistry, Bulgarian Academy of Sciences, Acad. G. Bonchev St., B1.11, 1113 Sofia, Bulgaria; stoychev@ipc.bas.bg
[4] Applied Nanometrix, LLC, P.O. Box 22396, Knoxville, TN 37933, USA; jennifer@appliednanometrix.net
* Correspondence: sabina_cherneva@yahoo.com; Tel.: +359-2-9796751

Abstract

Two nickel coatings—with plating-bath pH values of 3.8 and 4.8 and thicknesses of 9.38 μm and 4.88 μm, respectively—were chemically deposited onto ABS (acrylonitrile butadiene styrene) substrates with a thickness of 2040 μm. ABS is a plastic widely used as a structural material. Various types of components—formerly made of metal but now produced from ABS plastic to save metal and reduce structural weight—can be easily extruded or, in certain cases, molded. Nanoindentation experiments were conducted on the two nickel coatings and the ABS substrate using the XP head and CSM module of a G200 nanoindenter (KLA Corporation, Milpitas, CA, USA), alongside an "Express test" on the substrate. The substrate's influence on the film's indentation modulus was eliminated using the Hay-Crawford analytical model. Moreover, wear resistance tests were performed on the coatings, with the sample surfaces scanned using the NanoVision module both before and after the tests. The influence of the plating-bath pH on the mechanical properties of the investigated coatings was evaluated. It was found that with increasing plating-bath pH of films, their indentation hardness and indentation modulus decrease.

Keywords: electroless deposition; Ni; ABS; mechanical properties; nanoindentation; hardness; wear resistance

1. Introduction

ABS (Acrylonitrile butadiene styrene) is a thermoplastic polymer with an extremely wide range of applications as a construction material. It is very easy to extrude and, in certain cases, cast various types of parts that were previously made of metal, but are now made of ABS plastic to save metal and make the structure lighter. For example, most of the parts in a bathroom (decorative rings around faucets, shower sprayers, sink accessories—stoppers, soap dishes, chains, etc.) and everything that looks like chrome-plated metal are actually made of ABS plastic, on which a nickel coating is chemically deposited (for electrical purposes), after which copper, nickel, and chrome coatings are electrochemically deposited on it, which are much thicker and give the necessary decorative and protective effect. In addition, almost all accessories on the outside and inside of a car (emblems, inscriptions, etc.) are made of ABS plastic and then metallized. Other areas of application are microelectronics, household mechanical engineering, jewelry, etc. Among currently available plastics, ABS is becoming an obvious choice for deposition substrate due to its very

Check for updates

Academic Editor: Masato Sone

Received: 3 October 2026
Revised: 24 October 2026
Accepted: 26 October 2026
Published: 28 October 2026

Copyright: © 2026 by the authors. Licensee MDPI, Basel, Switzerland. This article is an open access article distributed under the terms and conditions of the Creative Commons Attribution (CC BY) license.

good adhesion to metals, low cost, low coefficient of thermal expansion, ease of molding, and good appearance after coating [1–4].

Electroless nickel plating (ENP) is the deposition of a nickel coating by chemical reduction, as opposed to the electric current used in electroplating processes. The advantages of electroless nickel plating are uniformity of the coating [5–9], high corrosion resistance and wear protection, uniform thickness, hardness and durability, the ability to be deposited on both metallic and non-metallic substrates, including plastics and ceramics, protection from harsh environmental conditions, etc. ENP has a wide range of applications in aerospace, oil and gas, and automotive manufacturing.

The pH level of the bath is one of the factors that has the greatest influence on the deposition rate, phosphorus content, surface morphology, and mechanical properties of electroless nickel coatings on ABS plastics. To initiate chemical deposition on ABS, the surface must be pretreated with etching and palladium activation, since ABS is a non-conductive polymer. Baths with a pH in the range of 4.0–5.5 lead to higher phosphorus content and smoother structures, while baths with a pH of 7.5–11.0 lead to increased deposition rate and gloss. At a pH range of 3.0–5.5, the plating speed is relatively slow [10]; moreover, high phosphorus incorporation (10–15% wt. P) occurs [11], which leads to an amorphous structure [12]. Electroless deposition at pH between 3 and 5.5 results in Ni coatings with excellent corrosion resistance due to the absence of grain boundaries. However, their microhardness and adhesion to the ABS substrate are lower than alkaline coatings due to slower initial nucleation [10].

There aren't many investigations of the influence of the pH of the bath on the mechanical properties of electroless-deposited metal coatings on ABS substrates. Such attempts have been made in works [13–16] with electroless-deposited copper coatings on ABS substrates, Ni–P alloy/MWCNT coatings [17], or Cu/MWCNT coatings [18]. Tsuru et al. investigated peeling strength and adhesive strength of electroless-deposited nickel coatings on ABS substrates [19], and Tengsuwan et al. made tensile tests and determined the tensile strength of the nickel coatings on ABS substrates [20]. We found only one article in the literature that investigated the influence of the same plating-bath pH as ours (3.8 and 4.8) on the hardness of the coating. This is publication [10]. Chakarova et al. deposited nickel-phosphorus coatings onto an ABS substrate by electroless deposition at the same pH of the bath, 3.8 and 4.8, like us, and obtained microhardness of the coatings, which is smaller than ours, probably because of the different electrolyte composition and different thickness of the coatings [10]. Moreover, they did not obtain the elastic modulus and wear resistance of the films. In our case, we obtained both the elastic modulus and the hardness by nanoindentation experiments and wear resistance by means of a wear test. We used our own method to obtain the substrate-independent elastic modulus, which has not been done in any other publication on the subject in the literature. The different composition of the electrolyte and the different plating-bath pH lead to a difference in the microstructure and, accordingly, in the mechanical properties of the coatings, practically resulting in a new material. This and the study of an elastic modulus independent of the properties of the substrate also constitute the novelty of the present study. Saroha et al. tried to improve the mechanical properties of the ABS substrate by electrodepositing a Ni coating. They found an improvement in the wear resistance and hardness after coating [21].

Sribalaji et al. performed nanoindentations and nanoscratch experiments on the as-deposited and annealed electroless nickel-phosphorus coating, deposited on a steel substrate [22]. They found an improvement of 32% in hardness and 31% in elastic modulus upon annealing the coating at 600 °C. They did not investigate the influence of the pH of the bath (the plating-bath pH in this work was 4.5–5.5) on the mechanical properties of the film and did not remove the influence of the substrate on the elastic modulus of the

film. Similar investigations of microstructure, hardness, corrosion, and wear behaviors of electroless NiP-TiC-SiC coating on ABS substrate were also made in work [23], where the authors found that to achieve the best hardness value for the film, a short deposition period (30 min) and high deposition rate (95 °C) are necessary. They also did not investigate the influence of the pH of the bath on the indentation hardness and modulus of the film.

Changes in the pH of an electroless nickel plating bath affect the composition, deposition rate, and structure of the nickel-phosphorus layer on an ABS plastic substrate, leading to changes in the layer's mechanical properties. That is why the present work aimed to investigate the influence of the plating-bath pH on the mechanical properties of electroless-deposited nickel coatings on an ABS substrate.

2. Materials and Methods

The investigated nickel layers were chemically deposited on ABS-polymer substrates with dimensions of 10 × 10 mm, cut from sheet material with a thickness of 2 mm. The nickel coating with a plating-bath pH of 3.8 had a thickness of 9.38 µm, and the nickel coating with a plating-bath pH of 4.8 had a thickness of 4.88 µm. The two Ni coatings were deposited under different bath pH values and further analyzed.

The pre-treatment of the ABS substrates was carried out according to the following technological scheme:

- pickling in a solution of bichrome mixture for 15 min at 65 °C and treatment in 3 M HCl for 3 min at room temperature;
- activation in a colloidal solution of $PdCl_2$ at room temperature for 5 min;
- acceleration in an alkaline solution at room temperature for 5 min
- Chemical nickel plating was carried out in a base solution containing the following components—Table 1.

Table 1. Electrolyte composition and conditions for electroless nickel plating.

Electrolyte Composition	Working Concentrations
$NiSO_4 \cdot 7H_2O$, g/L	10–30
$NaH_2PO_2 \cdot H_2O$, g/L	10–40
Complexing agents, g/L	5–50
Stabilizers, mg/L	0.5–20
Surfactants, g/L	0.01–0.6
pH	3.8–4.8
Temperature, °C	50–87

Chemical deposition was performed in a 250 mL bath under air agitation with an air flow of 100 mL/min/250 mL of electrolyte.

Nanoindentation experiments were performed on the two nickel coatings with different pH values, as well as on the ABS substrate with a G200 nanoindenter (KLA Corporation, Milpitas, CA, USA) equipped with an XP-head (with a Berkovich indenter with an angle of 136° and a 20 nm tip rounding) and a CSM module, using the "G-Series CSM Standard Hardness, Modulus, and Tip Cal" indentation method. In this method, the hardness and indentation modulus are obtained as a continuous function of the penetration into the surface of the tested material. In addition, the substrate was also tested using the Express test attachment of the NanoIndenter G200. The Express test allows for a high-speed nanoindentation experiment (100 indentations in 100 s), which allows avoiding the influence of time-dependent factors such as temperature, creep, etc.

Table 2 provides the input data for the nanoindentation experiments on the ABS substrate using the Express test option of the NanoIndenter G200.

Table 2. Input data for the nanoindentation experiments on the ABS substrate using the Express test attachment of the NanoIndenter G200.

Panel Inputs	Value	Units
Poisson's Ratio	0.3	-
Prescribed Displacement	1000	nm
Surface Approach Distance	0.05	nm
X Data Dimension	5	-
X Start Position	−50.000	µm
X Stop Position	50.000	µm
Y Data Dimension	5	-
Y Start Position	−50.000	µm
Y Stop Position	50.000	µm

Table 3 shows the input data for the nanoindentation experiments on the nickel coatings with pH = 4.8 and pH = 3.8, and the ABS substrate.

Table 3. Input data for the nanoindentation experiments on the nickel coatings and the ABS substrate.

Test	Surface Approach Velocity	Depth Limit	Strain Rate Target	Harmonic Displacement Target	Frequency Target	Surface Approach Distance	Poisson's Ratio
	nm/s	nm	1/s	nm	Hz	nm	
1	100	2000	0.05	2	45	10,000	0.3
2	100	2000	0.05	2	45	10,000	0.3
3	100	2000	0.05	2	45	10,000	0.3
4	100	2000	0.05	2	45	10,000	0.3
5	100	2000	0.05	2	45	10,000	0.3
6	100	2000	0.05	2	45	10,000	0.3
7	100	2000	0.05	2	45	10,000	0.3
8	100	2000	0.05	2	45	10,000	0.3
9	100	2000	0.05	2	45	10,000	0.3
10	100	2000	0.05	2	45	10,000	0.3
11	100	2000	0.05	2	45	10,000	0.3
12	100	2000	0.05	2	45	10,000	0.3

Then, the data obtained from the nanoindentation experiments for the nickel coatings were processed using the "G-Series CSM Hardness, Modulus for Thin Films" method, which separates the coating properties from the substrate properties, and the results are given in Figures 1–3. The input data for the nickel coatings with pH = 4.8 and pH = 3.8 are given in Tables 4 and 5, respectively. This yields the Young's modulus and the hardness of the coating as a continuous function of displacement [24]. The Young's modulus is corrected for the influence of the substrate using an analytical model, which is described in detail in [25–27]. To use this method, it is necessary to know the coating thickness, Young's modulus, and Poisson's ratio of the substrate. In addition, wear resistance tests were carried out on both nickel coatings using the G-Series Multi-Cycle Wear Test method. The input data for the wear resistance experiments of the nickel coatings with pH = 4.8 and pH = 3.8, respectively, are given in Tables 6 and 7, and the obtained results are shown in Figures 4 and 5 and Tables 8 and 9. The G-Series Multi-Cycle Wear Test Method is used to provide wear track deformation and per-cycle displacement averages for pass and return segments. Data are only recorded for the residual deformation of the wear track after each set of wear cycles. The cross-profile topography is also calculated (Figures 6 and 7). This method is intended for tests requiring 100 or more cycles (in our case, 100 wear cycles).

Before and after the tests, the surfaces of the samples were scanned by the NanoVision module (Figures 8 and 9).

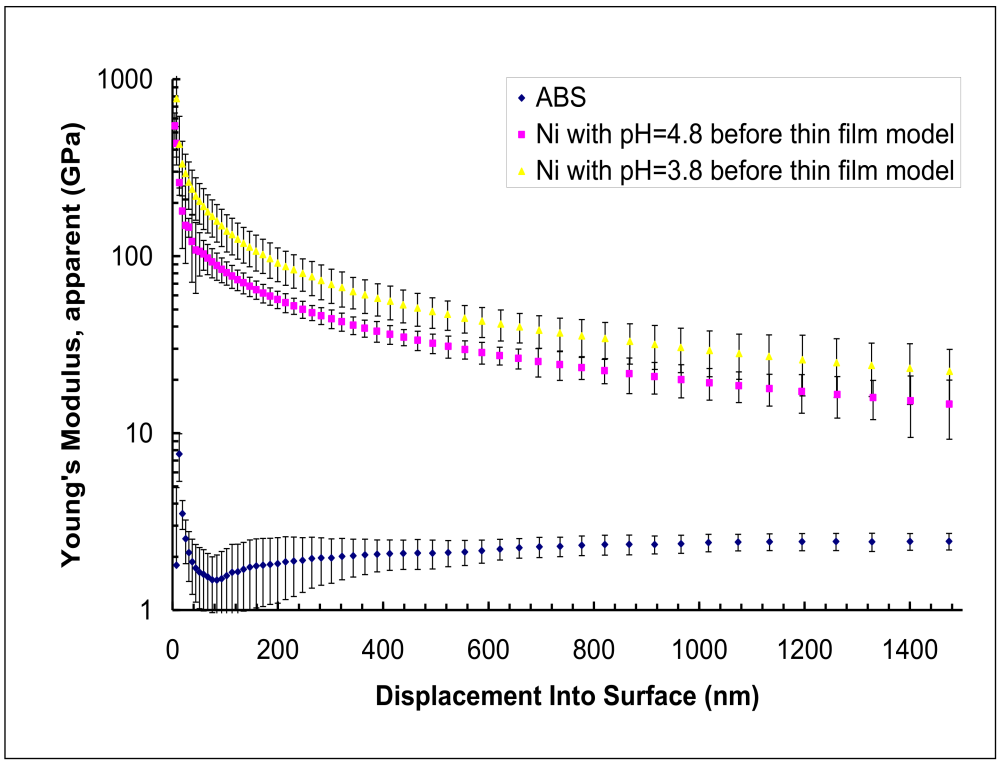


Figure 1. Young's modulus of the ABS substrate and the nickel coatings before application of the thin film model.

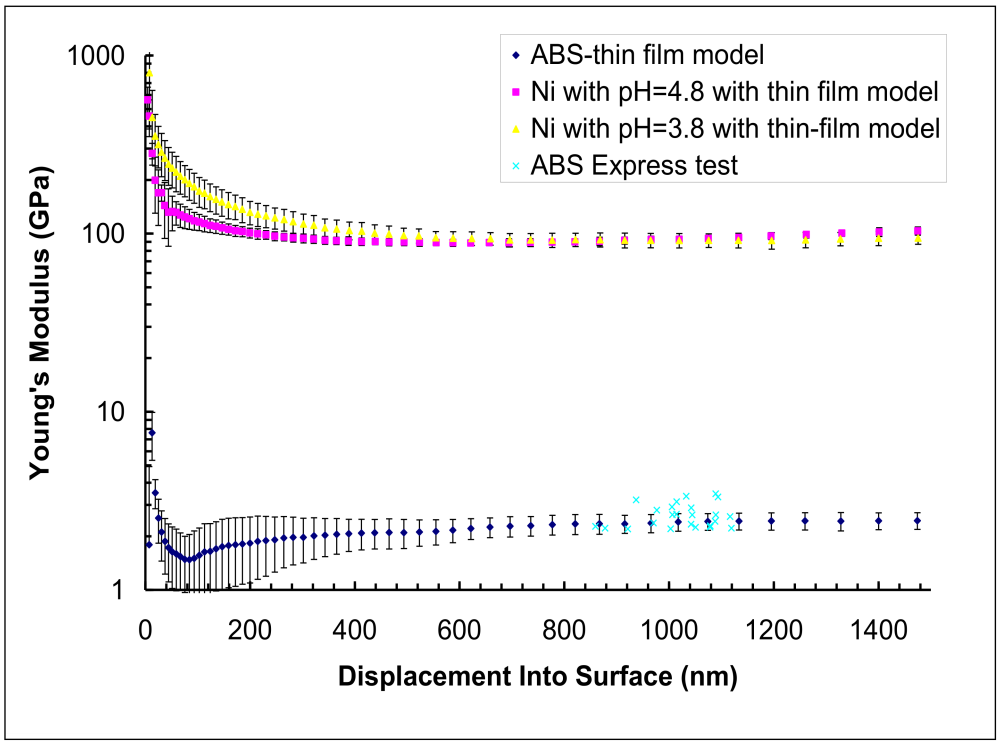


Figure 2. Young's modulus of the ABS substrate and the nickel coatings after application of the thin film model.

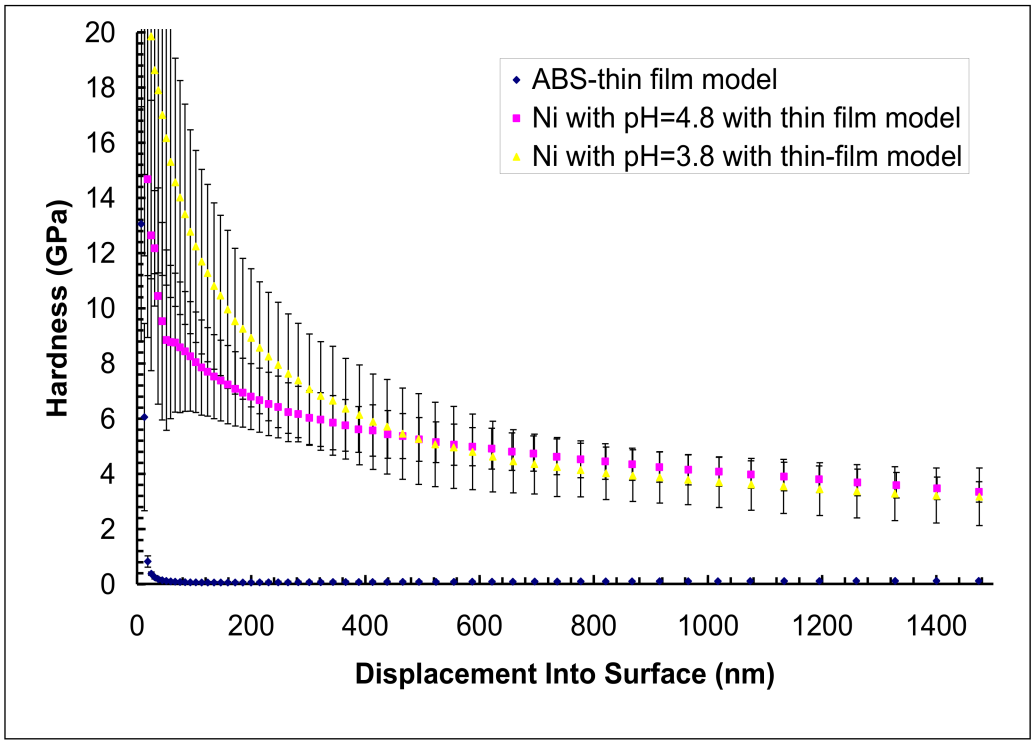


Figure 3. Results for the indentation hardness of coatings and the substrate.

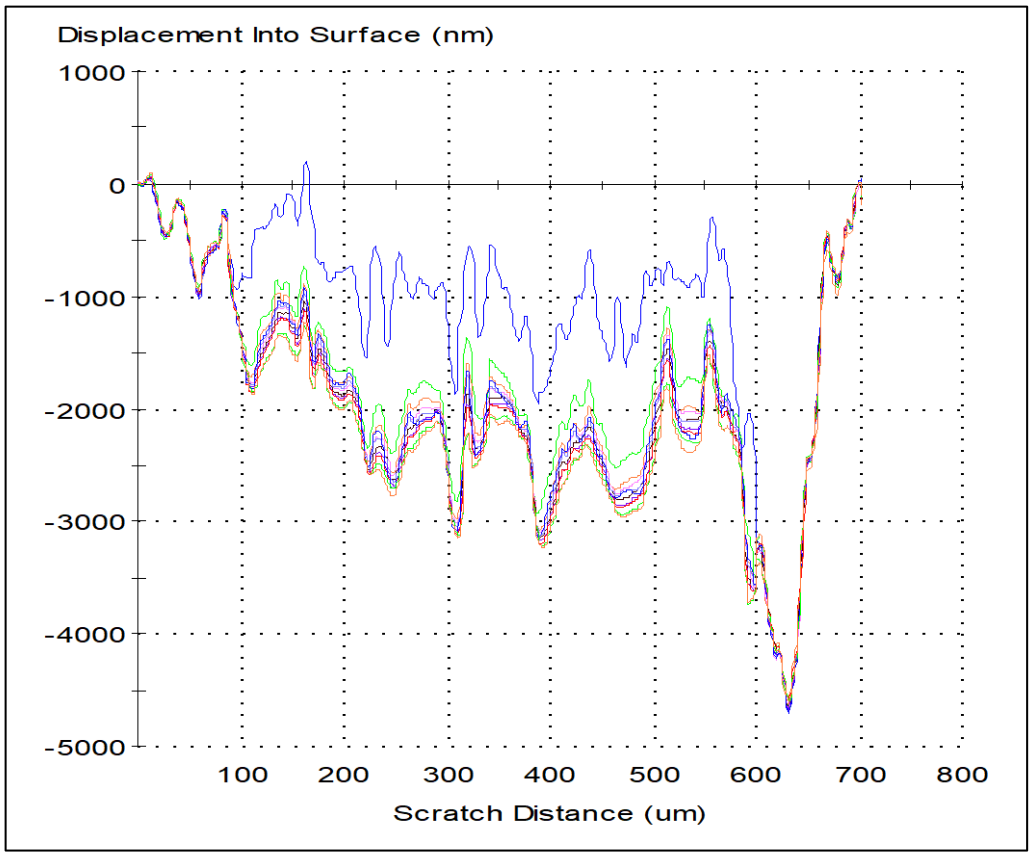


Figure 4. Results of wear resistance test of Ni coating with plating-bath pH= 4.8.

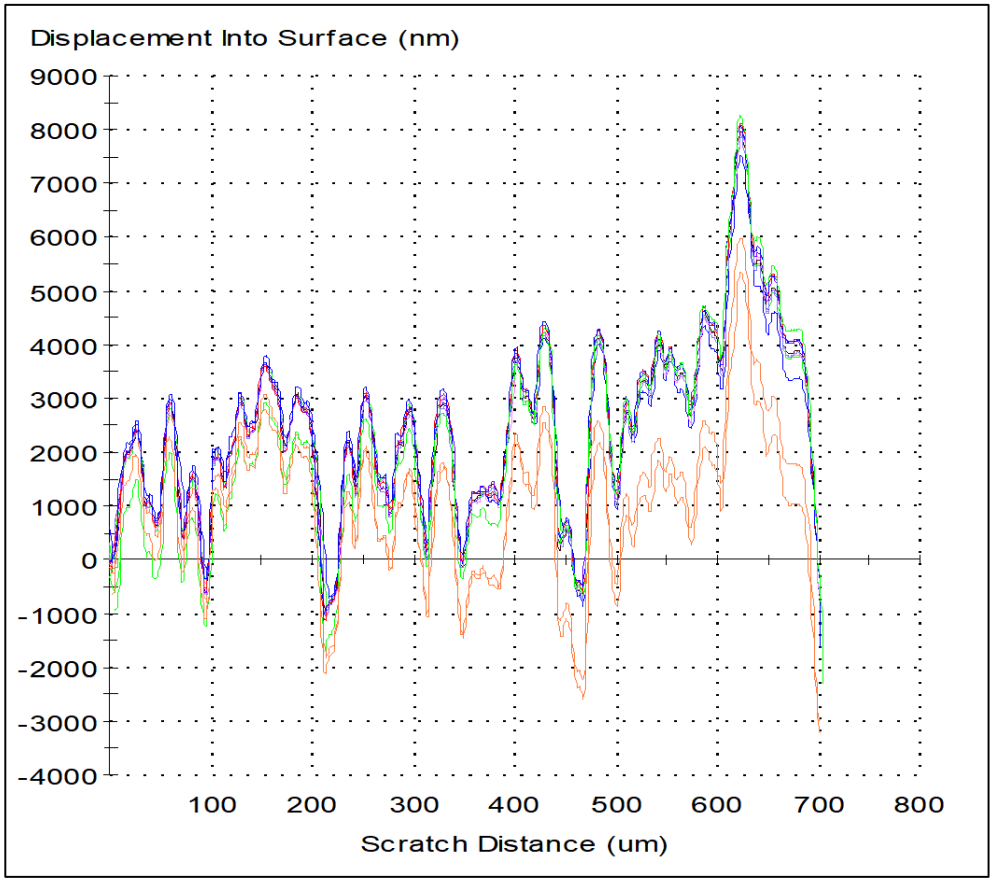


Figure 5. Results of wear resistance test of Ni coating with plating-bath pH = 3.8.

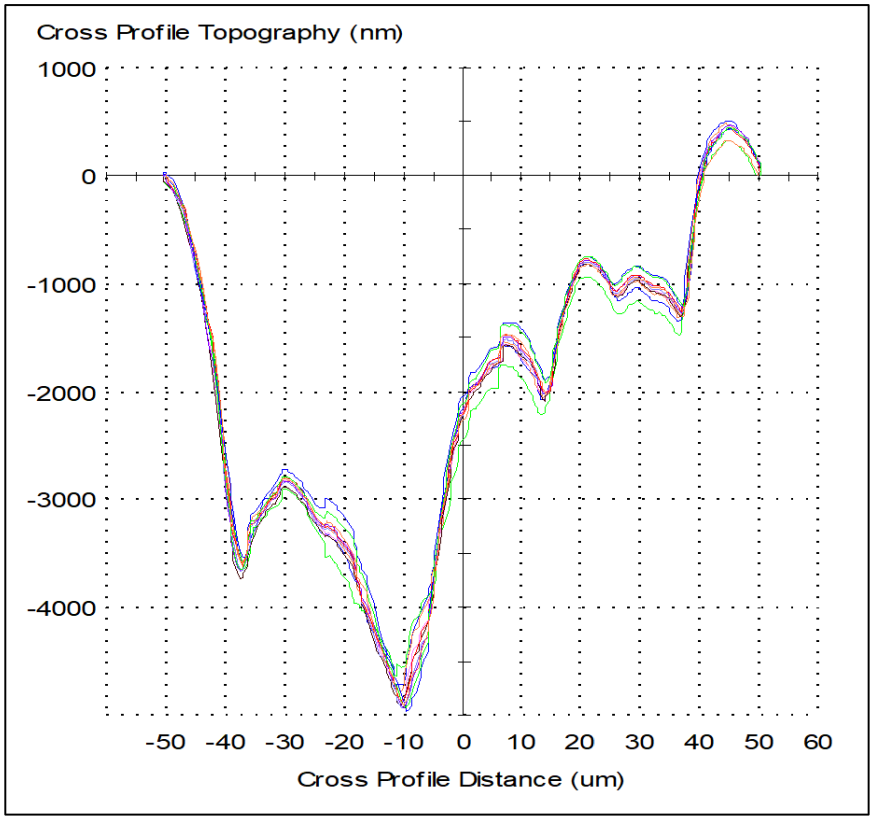


Figure 6. Cross profile topography for the Ni coating with plating-bath pH = 3.8.

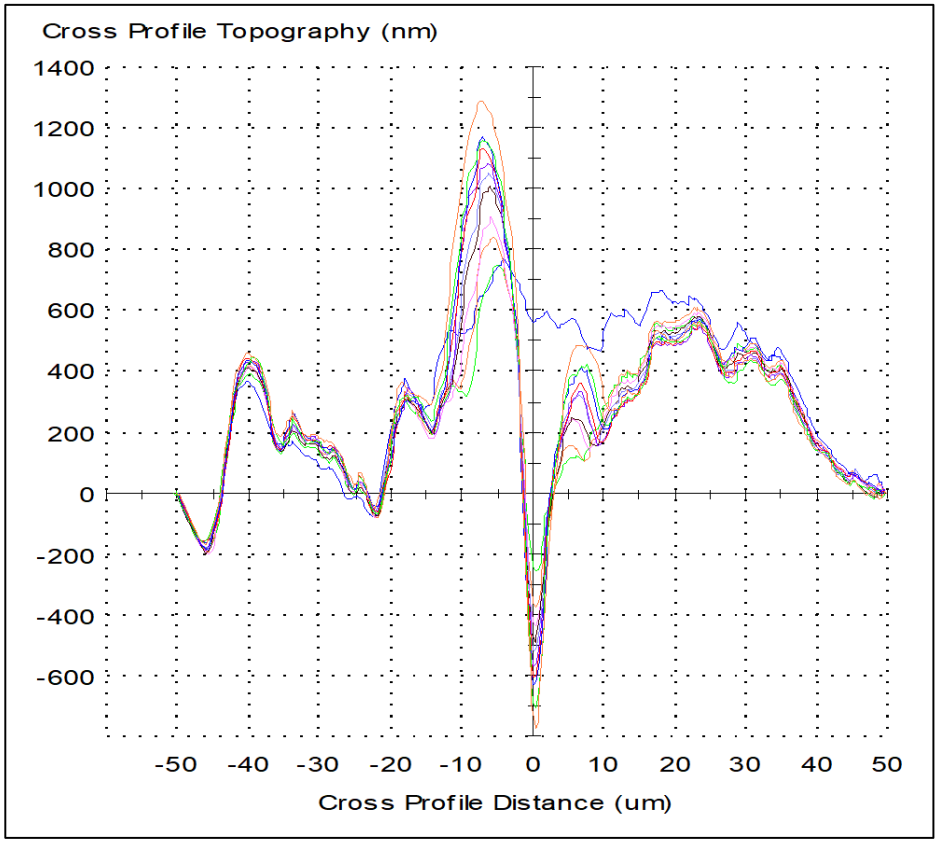


Figure 7. Cross profile topography for the Ni coating with plating-bath pH = 4.8.

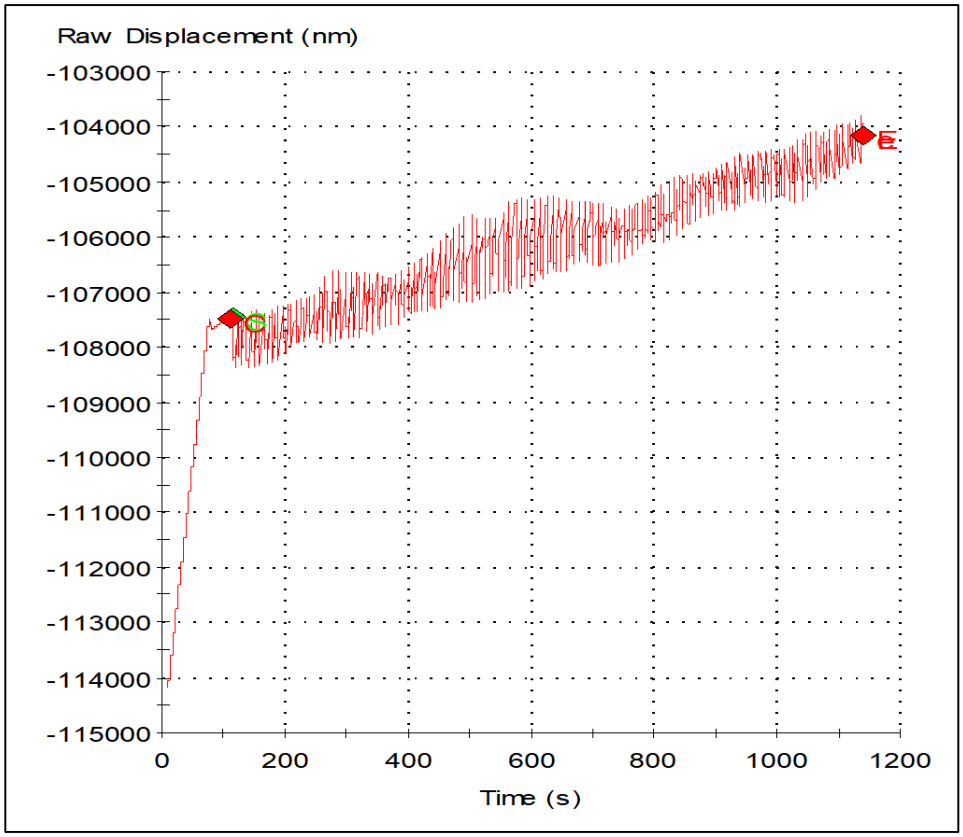


Figure 8. NanoVision scanned surface of Ni coating with plating-bath pH = 4.8 before wear resistance test.

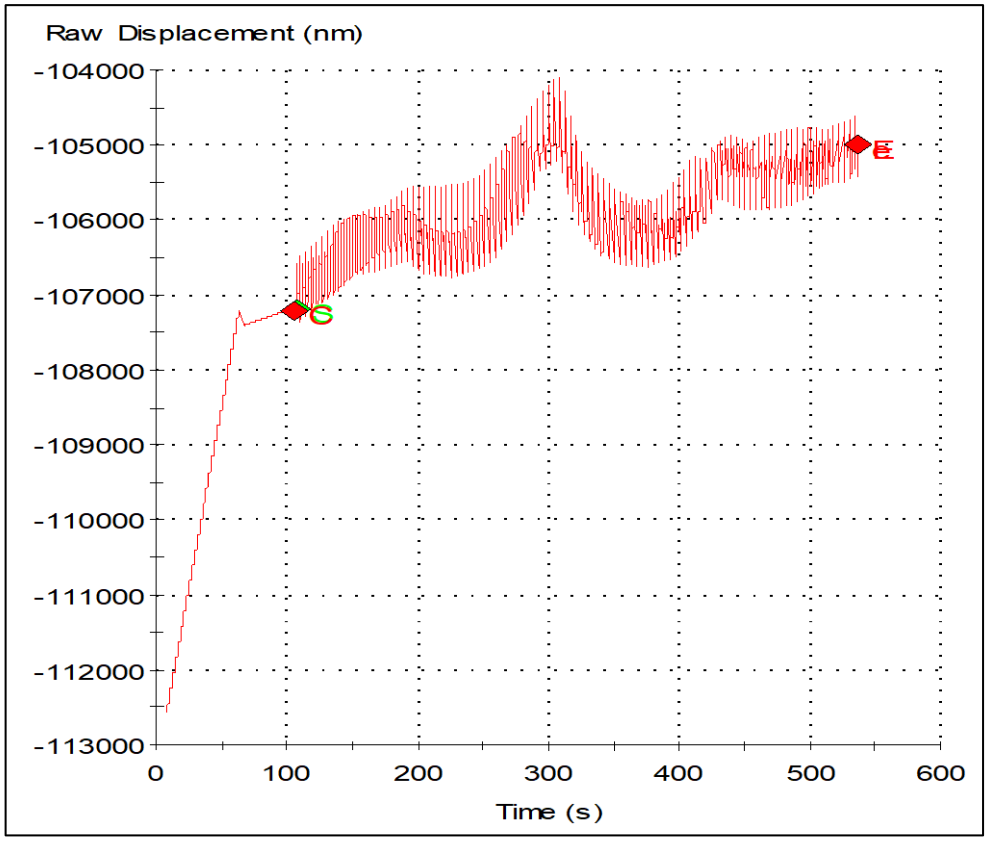


Figure 9. NanoVision scanned surface of Ni coating with plating-bath pH = 4.8 after wear resistance test.

Table 4. Input data for the "G-Series CSM Hardness, Modulus for Thin Films" method, which separates the coating properties from the substrate properties, used for the nickel coating with pH = 4.8.

Panel Inputs	Value	Units
Depth Limit	500	nm
Film or bulk (1 for film; 0 for bulk)	1	-
Film Thickness	4880	nm
Frequency Target	45	Hz
Harmonic Displacement Target	2	nm
Poisson's Ratio, film	0.3	-
Poisson's Ratio, substrate	0.3	-
Strain Rate Target	0.05	1/s
Surface Approach Detection Stiffness Criteria	100	N/m
Surface Approach Distance	1000	nm
Surface Approach Velocity	10	nm/s
Young's modulus, substrate	2.640	GPa

Table 5. Input data for the "G-Series CSM Hardness, Modulus for Thin Films" method, which separates the coating properties from the substrate properties, used for the nickel coating with pH = 3.8.

Panel Inputs	Value	Units
Depth Limit	500	nm
Film or bulk (1 for film; 0 for bulk)	1	-
Film Thickness	9380	nm
Frequency Target	45	Hz
Harmonic Displacement Target	2	nm

Table 5. *Cont.*

Panel Inputs	Value	Units
Poisson's Ratio, film	0.3	-
Poisson's Ratio, substrate	0.3	-
Strain Rate Target	0.05	1/s
Surface Approach Detection Stiffness Criteria	100	N/m
Surface Approach Distance	1000	nm
Surface Approach Velocity	10	nm/s
Young's modulus, substrate	2.640	GPa

Table 6. Input data for the wear resistance experiment for Ni coating with pH = 4.8.

Required Inputs	Value	Units
Wear Path Orientation	0	deg
Perform Cross Profile	1	(Integer)
Profiling Data Density (pts/µm)	1	(Integer)
Wear Track Data Density (points/µm)	1	(Integer)
Number of Wear Cycles (per Wear set)	10	(Integer)
Number of Wear Sets	10	(Integer)
Pre and Post Profile Lengths	20	%
Profiling Load	50	µN
Profiling Velocity	50	µm/s
Wear Test Velocity	50	µm/s
Wear Load	100	mN
Cross Profile Length	100	µm
Wear Path Length	500	µm

Table 7. Input data for the wear resistance experiment for Ni coating with pH = 3.8.

Required Inputs	Value	Units
Perform Cross Profile	1	(Integer)
Profiling Data Density (pts/µm)	1	(Integer)
Wear Track Data Density (points/µm)	1	(Integer)
Wear Load	5	mN
Number of Wear Cycles (per Wear Set)	10	(Integer)
Number of Wear Sets	10	(Integer)
Pre and Post Profile Lengths	20	%
Profiling Load	50	µN
Profiling Velocity	50	µm/s
Wear Test Velocity	50	µm/s
Wear Path Orientation	90	deg
Cross Profile Length	100	µm
Wear Path Length	500	µm

Table 8. Results of wear resistance test of Ni coating with plating-bath pH = 4.8.

Test	Cycle Comment	Completed Number of Wear Cycles	Wear Track Deformation	Maximum Wear Track Deformation	Per Cycle Average Displacement into Surface	Position for Cross Profile	Wear Track Width	Residual Groove Depth	Total Groove Height	Pile Up Height
			μm^2	μm^2	nm	µm	µm	nm	nm	nm
1				666.468		350				
1-1	Original Topography	0	0		−1125.73		-	-	-	-
1-2	Wear Cycle	10	453.57		−2092.71		28.6	255	918	662
1-3	Wear Cycle	20	529.78		−2262.11		28.8	376	1097	722
1-4	Wear Cycle	30	555.23		−2317.71		29.3	437	1187	750
1-5	Wear Cycle	40	585.52		−2378.38		29.4	493	1286	793
1-6	Wear Cycle	50	563.36		−2337.8		29.7	521	1335	814
1-7	Wear Cycle	60	609.64		−2423.81		29.9	570	1385	815
1-8	Wear Cycle	70	618.51		−2444.47		30.3	607	1449	842
1-9	Wear Cycle	80	560.83		−2336.17		30.4	631	1501	870
1-10	Wear Cycle	90	658.35		−2511.79		30.3	705	1565	860
1-11	Wear Cycle	100	666.47		−2528.4		30.4	774	1699	925

Table 9. Results of wear resistance test of Ni coating with plating-bath pH = 3.8.

Test	Cycle Comment	Completed Number of Wear Cycles	Wear Track Deformation	Maximum Wear Track Deformation	Per Cycle Average Displacement into Surface	Position for Cross Profile	Wear Track Width	Residual Groove Depth	Total Groove Height	Pile Up Height
			μm^2	μm^2	nm	µm	µm	nm	nm	nm
1				693.768		350				
1-1	Original Topography	0	0		1757.456		-	-	-	-
1-2	Wear Cycle	10	−31.10		1799.07		95.6	4637	4796	159
1-3	Wear Cycle	20	693.77		360.01		94.3	4785	5029	243
1-4	Wear Cycle	30	14.89		1742.10		95.5	4878	5110	232
1-5	Wear Cycle	40	−4.10		1710.44		95.5	4916	5132	215
1-6	Wear Cycle	50	30.97		1662.09		95.3	4933	5146	212
1-7	Wear Cycle	60	−14.99		1768.85		95.4	4930	5166	236
1-8	Wear Cycle	70	−37.58		1774.63		94.9	4858	5078	220
1-9	Wear Cycle	80	−52.20		1870.82		95.3	4960	5191	232
1-10	Wear Cycle	90	170.23		1450.86		94.8	4933	5155	222
1-11	Wear Cycle	100	644.49		444.00		95	4919	5084	164

3. Results and Discussion

We selected electroless nickel plating because of the following advantages: it produces uniform coatings that cover complex shapes and secure good adhesion to the substrate; it imparts a metallic appearance, enhanced wear resistance, and electrical conductivity to the plastic. Furthermore, electroless nickel plating is widely used in mechanical engineering and the automotive industry, in electronics and precision mechanics, and in the oil and gas sector for components exposed to aggressive environments, among other applications.

Usually, the Oliver and Pharr approximation method [28] is used to extract the indentation modulus and hardness of the films after nanoindentation experiments. In cases where the elastic modulus of the coating is more than twice that of the substrate, the Oliver-Pharr method does not work well. In such instances, it is highly appropriate to apply the Hay-Crawford method. The Hay–Crawford method was published in our previous work [26], but was applied in the present study to obtain substrate-independent properties of the system Ni coating-ABS substrate. The depth limit of this method is 500 nm, because the Hay-Crawford model always improves the accuracy of Young's modulus within the domain of $h/t < 25\%$. The results obtained before and after its application are presented in Figures 1–3.

Because ABS is a soft polymer substrate (with low modulus), accurate measurement of the thin nickel coating's true elastic modulus requires ultra-shallow nanoindentation, acoustic methods, or analytical methods to eliminate underlying plastic deformation effects. In our case, we used a 2000 nm depth limit during the nanoindentation experiment, and then we used the analytical method of Hay-Crawford in order to extract the substrate-independent elastic modulus of the nickel films. The model works well for stiff films on soft substrates and also for soft films on stiff substrates. In our case, we have a much harder coating on a softer substrate. Typically, with hard films on soft substrates—as is the case here—excessive sinking-in is observed; this can lead to an artificially low Young's modulus due to the calculation of overly large contact areas [26].

Figure 1 shows that before using the Hay-Crawford model to obtain a substrate-independent elastic modulus of the coating, the modulus of the two nickel coatings obtained at different plating-bath pH values decreases with increasing indenter penetration depth, due to the influence of the ABS substrate, which, as can be seen from the same figure, has a much smaller elastic modulus than that of the coatings.

Applying the Hay-Crawford model eliminates the influence of the substrate on the coating's elastic modulus; as shown in Figure 2, the elastic modulus becomes constant (91.88 GPa for the nickel film with plating-bath pH = 3.8 and 89.61 GPa for the nickel film with pH = 4.8)—and higher than the value obtained experimentally. The standard deviation of the elastic modulus is 8.63 GPa for the nickel film with pH = 3.8 and 4.14 GPa for the nickel film with pH = 4.8. The model cannot eliminate the influence of the substrate on the hardness, and the hardness decreases as the indentation depth increases, as shown in Figure 3. The Hay–Crawford method does not remove substrate effects from hardness, but improves it; that is why the hardness comparison is used to infer a general pH dependence.

The Indirect Improvements to the Hardness Data are the following:

While the model does not change the hardness formula itself, it drastically improves the reliability of concurrent hardness data collection in two main ways:

- Enables Deeper Indentations: Traditional thin-film testing relies on the "10% rule" (indenting no deeper than 10% of the film thickness to avoid substrate interference). By using the Hay-Crawford model, users can confidently indent much deeper—up to 20% to 40% of the film thickness—to get clean elastic data.
- Reduces Data Noise: Testing at 20% film thickness allows the material's hardness to reach a stable plateau where substrate influence is naturally negligible. Deeper indents

bypass the severe errors typically caused by surface roughness, environmental noise, and indenter tip anomalies that distort shallow (under 10 nm) data. The standard deviation of the indentation hardness is 0.91 GPa for the nickel film with pH = 3.8 and 0.79 GPa for the nickel film with pH = 4.8. The indentation hardness and indentation modulus of both coatings at small depths of indentation have higher experimental error because of the imperfections of the tip of the indenter, as well as being influenced by the roughness of the sample surface [29,30]. From Figure 2, it can be seen that the results for the indentation modulus of the substrate obtained by the so-called Express test, which allows avoiding the influence of time-dependent factors such as temperature, creep, etc., are similar to those from the thin-film model. The Express Test option by KLA Instruments is a high-speed nanomechanical testing mode designed to map and measure surface properties rapidly with minimal thermal drift. The Express Test option for G200 NanoIndenters implements traditional indentation testing in a revolutionary way to achieve unprecedented testing speeds. Express Test performs one complete indentation cycle per second, including approach, contact detection, load, unload, and movement to the next indentation site. One hundred indentations can be performed at one hundred different sites in less than 100 s. The benefits which follow from this capability are myriad, but the most obvious are rapid calibration of indenter area function and statistically robust measurement of hardness and Young's modulus in mere minutes. Because testing is so fast, thermal drift is inconsequential. In summary, the Express Test option increases the productivity of a G200 NanoIndenter more than a hundredfold [31].

From Figures 2 and 3, it can be seen that the indentation hardness and modulus of the ABS substrate coated with nickel coatings with different plating-bath pH are much higher than those of the uncoated substrate. Moreover, increasing the pH of the electrolyte leads to a decrease in the indentation hardness and indentation modulus. One possible reason for the decrease in the indentation modulus is that as bath pH increases, the phosphorus co-deposition rate changes, lowering the elastic modulus for high-phosphorus amorphous films. This is a well-documented mechanism in the material science of electrodeposited coatings, particularly for electroless or electroplated nickel-phosphorus (Ni-P) alloys. [32]. The decrease in indentation hardness can be explained by the well-known inverse Hall-Petch effect—below a critical grain size, hardness decreases with decreasing grain size [33]. Another possible reason for the obtained result is the co-deposition of hydroxides. The results obtained by us for the Young's modulus and hardness of the uncoated ABS substrate are in good agreement with those obtained from Saroha et al. in their work [21]. They used electrochemical deposition of Ni coatings, not electroless deposition, and also different pH values of the bath (3.6, 4.5 and 5.5); that is why we couldn't compare their results for the indentation hardness and modulus of the nickel coatings with our results. Czagany et al. also investigated the influence of the plating-bath pH on the mechanical properties of Ni-P coatings, but on a different substrate (W302 steel substrate) and different pH values (4.2, 5.2, 6.2, 7.2, 8.2, 9.2) [34]. Chakarova et al. deposited nickel-phosphorus coatings onto an ABS substrate by electroless deposition at the same pH of the bath, 3.8 and 4.8, like us, and obtained microhardness of the coatings, which is smaller than ours, probably because of the different electrolyte composition and different thickness of the coatings, which leads to different microstructure and mechanical properties of the coatings [10]. They did not obtain the elastic modulus and wear resistance of the coatings. They found that for the same deposition time, the thickness of the coating deposited in an electrolyte with pH 3.8 is twice smaller than that obtained at pH 4.8. Moreover, they found that with an increase in the electrolyte pH, the thickness of the Ni coatings increases. We obtained that the maximum wear track deformation of the Ni coating with pH = 4.8 was smaller than that of the Ni coating with pH = 3.8 (Tables 8 and 9), probably because the displacements into the surface

during the wear cycles were higher than 400 nm (see Figures 4 and 5), whereas we can see from Figure 3 that there is an influence of the substrate, and because of this influence the hardness of the Ni coating with pH = 4.8 became higher than the hardness of the Ni coating with pH = 3.8. We see that after 100 wear cycles, the coating surface had worn away, exposing the substrate—as evidenced by the peaks at displacement into the surface during the measurement equal to the coating thickness shown in Figures 4 and 5.

The cross-profile topography of the Ni coatings with plating-bath pH = 3.8 and 4.8 is shown in Figures 6 and 7. We see that the pile-up height of the Ni coating with pH = 4.8 is significantly greater than that of the nickel coating deposited at plating-bath pH = 3.8.

Scanning with the NanoVision nanoindenter attachment before and after the wear resistance test, shown in Figures 8 and 9, provides information about the surface topography of the coatings.

4. Conclusions

In the present work, nickel coatings with pH 3.8 and 4.8 were chemically deposited on an ABS substrate. The mechanical properties of the coatings and the substrate were obtained using nanoindentation and wear experiments. The influence of the bath pH on the mechanical properties of the obtained coatings was studied. Using the Hay-Crawford method, the substrate-independent indentation modulus of the two nickel coatings was obtained. The results showed that both nickel coatings significantly improved the mechanical properties of the ABS substrate. Furthermore, we found that as the plating-bath pH increases, indentation hardness and modulus decrease, while wear resistance increases. This result is of great importance for many applications, such as in the automotive industry, electronics and household appliances, sanitary ware and fittings, modeling and 3D printing.

Author Contributions: Conceptualization, S.C. and D.S.; methodology, J.H.; software, J.H.; validation, S.C., D.S. and J.H.; formal analysis, S.C.; investigation, S.C.; resources, D.S. and J.H.; data curation, S.C.; writing—original draft preparation, S.C.; writing—review and editing, D.S. and J.H.; visualization, S.C.; supervision, D.S.; project administration, S.C.; funding acquisition, S.C. All authors have read and agreed to the published version of the manuscript.

Funding: This work was supported by the European Regional Development Fund under the "Research Innovation and Digitization for Smart Transformation" program 2021–2027 under the Project BG16RFPR002-1.014-0006 "National Centre of Excellence Mechatronics and Clean Technologies". This research was also supported by the National Science Fund under Grant No.КП-06-H83/8 from 6 December 2024.

Institutional Review Board Statement: Not applicable.

Informed Consent Statement: Not applicable.

Data Availability Statement: The original contributions presented in this study are included in the article. Further inquiries can be directed to the corresponding author.

Conflicts of Interest: Author Jennifer Hay was employed by the company Applied Nanometrix. The remaining authors declare that the research was conducted in the absence of any commercial or financial relationships that could be construed as a potential conflict of interest.

Abbreviations

The following abbreviations are used in this manuscript:

ABS	Acrylonitrile butadiene styrene
CSM	Continuous Stiffness Measurement
ENP	Electroless nickel plating
pH	Potential of hydrogen

References

1. Olivera, S.; Muralidhara, H.B.; Venkatesh, K.; Gopalakrishna, K.; Vivek, S. Plating on acrylonitrile–butadiene–styrene (ABS) plastic: A review. *J. Mater. Sci.* **2016**, *51*, 3657–3674. [CrossRef]
2. Gupta, N.K.; Pandey, P.; Mehta, S.; Swati, S.; Mishra, S.K.; Tom, K.J. Characterization of ABS material in hybrid composites: A review. In *Advances in Engineering Design: Select Proceedings of FLAME*; Springer: Singapore, 2018; pp. 619–630. [CrossRef]
3. Lapčík, L.; Vašina, M.; Murtaja, Y.; Sepetcioglu, H.; Lapčíková, B.; Ovsík, M.; Staněk, M.; Karagöz, İ.; Vadanagekar, A.S. ABS Nanocomposites for Advanced Technical and Biomedical Applications. *Polymers* **2025**, *17*, 909. [CrossRef] [PubMed]
4. Vishwakarma, S.K.; Pandey, P.; Gupta, N.K. Characterization of ABS material: A review. *J. Res. Mech. Eng.* **2017**, *3*, 13–16.
5. Chintada, V.B.; Koona, R.; Raju Bahubalendruni, M.V.A. State of the Art Review on Nickel-Based Electroless Coatings and Materials. *J. Bio Tribo Corros.* **2021**, *7*, 134. [CrossRef]
6. Krishnan, K.H.; John, S.; Srinivasan, K.N.; Praveen, J.; Ganesan, M.; Kavimani, P.M. An overall aspect of electroless Ni-P depositions—A review article. *Metall. Mater. Trans. A* **2006**, *37*, 1917–1926. [CrossRef]
7. Sahoo, P.; Das, S.K. Tribology of electroless nickel coatings–a review. *Mater. Des.* **2011**, *32*, 1760–1775. [CrossRef]
8. Wang, C.; Zhai, H.; Lewis, D.; Gong, H.; Liu, X.; Fernando, A. Solvent-driven electroless nickel coatings on polymers: Interface engineering, microstructure, and applications. *Coatings* **2025**, *15*, 898. [CrossRef]
9. Kim, N.K.; Kang, S.M.; Kim, T.; Kim, S.; Kim, G.H. Electroless plating on polymer surfaces: Comprehensive review of mechanism, process, analysis, and future applications. *Adv. Mater. Interfaces* **2025**, *12*, 2400931. [CrossRef]
10. Chakarova, V.; Georgieva, M.; Petrova, M. Corrosion resistance of electroless deposited Ni-P coatings on polymer (ABS) substrate. *Bulg. Chem. Commun.* **2017**, *49*, 30–36.
11. Azli, N.N.A.; Mohd Amin, N.F.; Oluhende, S.T.; Mohamad, S.N.A.; Fadil, N.A. Electroless deposited black nickel-phosphorus solar absorber coatings on carbon steel: Effect of plating bath pH. *Mater. Today Proc.* **2021**, *39*, 1071–1076. [CrossRef]
12. Shaikh, M.S.N.M.; Ahuja, B.B. Optimization of Electroless Nickel Tungsten Composite Coating on 3D-Printed ABS Substrate for Maximum Tungsten Content. *J. Inst. Eng. India Ser.* **2022**, *C103*, 69–82. [CrossRef]
13. Yang, Z.; He, Y.; Li, Z.; Li, N.; Wang, Z. Adhesion improvement of ABS resin to electroless copper by H_2SO_4–MnO_2 colloid with ultrasound-assisted treatment. *J. Adhes. Sci. Technol.* **2011**, *25*, 1211–1221. [CrossRef]
14. Li, Z.; Li, N.; Yin, L.; He, Y.; Wang, Z. An environment-friendly surface pretreatment of ABS resin prior to electroless plating. *Electrochem. Solid-State Lett.* **2009**, *12*, D92–D95. [CrossRef]
15. Ma, Q.; Zhao, W.; Li, X.; Li, L.; Wang, Z. Study of an environment-friendly surface pretreatment of ABS-polycarbonate surface for adhesion improvement. *Int. J. Adhes. Adhes.* **2013**, *44*, 243–249. [CrossRef]
16. Shu, Z.; Wang, X. Environment-friendly Pd-free surface activation techniques for ABS surface. *Appl. Surf. Sci.* **2012**, *258*, 5328–5331. [CrossRef]
17. Arai, S.; Sato, T.; Endo, M. Fabrication of various electroless Ni–P alloy/multiwalled carbon nanotube composite films on an acrylonitrile butadiene styrene resin. *Surf. Coat. Technol.* **2011**, *205*, 3175–3181. [CrossRef]
18. Arai, S.; Kanazawa, T. Electroless deposition and evaluation of Cu/multiwalled carbon nanotube composite films on acrylonitrile butadiene styrene resin. *Surf. Coat. Technol.* **2014**, *254*, 224–229. [CrossRef]
19. Tsuru, Y.; Mochinaga, K.; Ooyagi, Y.; Foulkes, F.R. Application of vapor-deposited carbon and zinc as a substitute for palladium catalyst in the electroless plating of nickel. *Surf. Coat. Technol.* **2003**, *169*, 116–119. [CrossRef]
20. Tengsuwan, S.; Ohshima, M. Environmentally benign electroless nickel plating using supercritical carbon-dioxide on hydrophilically modified acrylonitrile–butadiene–styrene. *Appl. Surf. Sci.* **2014**, *311*, 189–200. [CrossRef]
21. Saroha, V.; Pabla, B.S.; Bhogal, S.S. Characterization of ABS for enhancement of mechanical properties. *Int. J. Innov. Technol. Explor. Eng.* **2019**, *8*, 2164–2167. [CrossRef]
22. Sribalaji, M.; Asiq Rahman, O.S.; Laha, T.; Keshri, A.K. Nanoindentation and nanoscratch behavior of electroless deposited nickel-phosphorus coating. *Mater. Chem. Phys.* **2016**, *177*, 220–228. [CrossRef]
23. Alhamad, R.K.; Hussein, A.K.; Abbas, L.K. Microstructure, Corrosion and Wear Behaviors of Electroless (NiP-TiC-SiC) Nanocomposite Coating on Acrylonitrile Butadiene Styrene Substrate. *Surfaces* **2024**, *7*, 1029–1051. [CrossRef]
24. Hay, J.L.; Agee, P.; Herbert, E.G. Continuous stiffness measurements during instrumented indentation testing. *Exp. Tech.* **2010**, *34*, 86–94. [CrossRef]
25. Hay, J.L. Measuring Substrate-Independent Young's Modulus. Agilent Technologies Application Note. 2010. Available online: https://assets.toyo.co.jp/files/user/img/product/microscopy/pdf/5990-6507EN.pdf (accessed on 24 October 2026).
26. Hay, J.; Crawford, B. Measuring substrate-independent modulus of thin films. *J. Mater. Res.* **2011**, *26*, 727–738. [CrossRef]
27. Hay, J. Measuring Substrate-Independent Young's Modulus of Thin Films. In *MEMS and Nanotechnology*; Proulx, T., Ed.; Conference Proceedings of the Society for Experimental Mechanics Series; Springer: New York, NY, USA, 2011; Volume 4. [CrossRef]
28. Oliver, W.C.; Pharr, G.M. An improved technique for determining hardness and elastic modulus using load and displacement sensing experiments. *J. Mater. Res.* **1992**, *7*, 1564–1583. [CrossRef]

29. Shafirstein, G.; Gee, M.G.; Osgerby, S.; Saunders, S.R.J. Error Analysis In Nanoindentation. *Mater. Res. Soc. Symp. Proc.* **1994**, *356*, 717–721. [CrossRef]
30. Menčík, J. Uncertainties and Errors in Nanoindentation. *Nanoindent. Mater. Sci.* **2012**, *54*, 53–86. [CrossRef] [PubMed]
31. Express Test Option for the Nano Indenter® G200, KLA Corporation, One Technology Drive, Milpitas, USA, CA 95035. Available online: https://www.kla-instruments.cn/wp-content/uploads/2022/06/KLA_OptionsDataSheet_ExpressTest.pdf (accessed on 24 October 2026).
32. Czagány, M.; Baumli, P.; Kaptay, G. The influence of the phosphorous content and heat treatment on the nano-micro-structure, thickness and micro-hardness of electroless Ni-P coatings on steel. *Appl. Surf. Sci.* **2017**, *423*, 160–169. [CrossRef]
33. Carlton, C.E.; Ferreira, P.J. What is behind the inverse Hall–Petch effect in nanocrystalline materials? *Acta Mater.* **2007**, *55*, 3749–3756. [CrossRef]
34. Czagany, M.; Baumli, P. Effect of Ph on the characteristics of electroless Ni-P coatings. *J. Min. Metall. Sect. B-Metall.* **2017**, *53*, 327–332. [CrossRef]

Disclaimer/Publisher's Note: The statements, opinions and data contained in all publications are solely those of the individual author(s) and contributor(s) and not of MDPI and/or the editor(s). MDPI and/or the editor(s) disclaim responsibility for any injury to people or property resulting from any ideas, methods, instructions or products referred to in the content.